

Time-dependent damage evolution and failure in materials. II. Simulations

W. A. Curtin and M. Pamel

Engineering Science and Mechanics, Virginia Polytechnic Institute and State University, Blacksburg, Virginia 24061

H. Scher

Department of Environmental Sciences and Energy Research, Weizmann Institute of Science, Rehovot, Israel

(Received 13 May 1996; revised manuscript received 6 November 1996)

A two-dimensional triangular spring network model is used to investigate the time-dependent damage evolution and failure of model materials in which the damage formation is a nucleated event. The probability of damage formation $r_i(t)$ at site i at time t is taken to be proportional to the local stress at site i raised to a power: $r_i(t) = A\sigma_i(t)^\eta$. As damage evolves in the material, the stress state becomes heterogeneous and drives preferential damage evolution in regions of high stress. As predicted by an analytical model and observed in previous electrical fuse network simulations, there is a transition in the failure behavior at $\eta=2$: for $\eta \leq 2$, the failure time and damage density are independent of the system size; for $\eta > 2$, the failure time and damage decrease with increasing time and failure occurs by the formation of a finite critical damage region which rapidly propagates across the remainder of the material. The stress distribution prior to failure exhibits no abrupt changes or scalings that indicate imminent failure. The scalings of the failure time and the failure time distribution are investigated, and compared with analytic predictions. The failure time scales as a power law in $\ln N_T$, where N_T is the system size, but the exponent is not the predicted value of $1-\eta/2$; this is attributed to a difference in the stress concentration factors (scf) between the discrete lattice and a continuum model. Using the scf values for the lattice lead to predicted scalings consistent with the simulations. Predicted absolute failure times versus size are generally in good agreement with simulation results at larger η values. The coefficient of variation of the failure time distribution is observed to be nearly constant, in slight contrast to the predicted scaling of $(\ln N_T)^{-1}$. Overall, the simulation results quantitatively and qualitatively validate many of the critical predictions of the analytic model. [S0163-1829(97)04017-4]

I. INTRODUCTION

The evolution of damage in a material, culminating in failure of the material after some time at load, is of great importance in the design of structural systems. Structural components are constructed to operate at stresses well below the fast-fracture strength of the component, and hence failure usually occurs in time due to cyclic or static fatigue mechanisms. The mechanisms of damage formation, accumulation, and ultimate failure can vary widely among different materials, but generally the damage formation rate is a nonlinear function of the applied stress, and the time to failure is a highly stochastic variable. It is therefore of considerable interest and practical use to develop a general understanding of the coupling of microscopic damage to macroscopic failure, and in particular, of the specific time scales for failure and their detailed statistical distributions. The latter is necessary to establish reliability of the material, and hence ultimately sets the limits on design stresses in an engineering application.

We have discussed previously the problem of failure under constant applied stress in a material for which the damage is a nucleated phenomenon with a damage rate that is dependent on the local stress at any time.^{1,2} Specifically, the relative probability of failure $r_i(t)$ at a damage site i at time t is assumed to be

$$\begin{aligned} r_i(t) &= A\sigma_i(t)^\eta \quad \sigma_i(t) > 0 \\ &= 0 \quad \sigma_i(t) < 0, \end{aligned} \quad (1)$$

where $\sigma_i(t)$ is the local stress on site i at time t and damage is presumed to occur only under tensile stress. Here, η is a parameter which accounts for the nonlinear relationship between damage rate and stress, and a power-law dependence is chosen to obtain often-observed power-law creep rates in the material at short times. In a companion publication, we have described the behavior of a Si/SiC composite which suggests the basic underlying damage rate law studied here. In addition, the present nucleated damage law is the simplest form possible, with no dependence on the prior stress history. However, even in the absence of memory effects, the failure of the material is complex and sensitive to the precise value of η . Analytic predictions of damage evolution, strain versus time, and the failure time distributions for this nucleated damage rate law exhibit some very subtle scalings of the time-dependent behavior for larger values of the nonlinearity parameter η .

In this paper, we present results obtained from computer simulations on the damage evolution and failure in spring network models which obey the damage rate law of Eq. (1), and compare the simulation results to the analytic predictions² in considerable detail. The numerical study confirms the overall predictions of the analytic model: a transition in failure behavior around $\eta=2$; more abrupt and less predictable failure as η increases; failure time decreasing as a power law of the logarithm of the system size; a width of the failure time distribution decreasing very slowly with increasing size. In detail, the exponents of the power-law dependence on $\ln(\text{size})$ are not quite as predicted in the analytic

model, but this is largely attributable to the slightly complex stress-concentration factors around small cracks in the discrete spring network. Also at $\eta=4$ (a low value but above the transition value) the importance of damage one next neighbor away from preexisting damage, followed by linking of the damage to form larger clusters, appears to drive failure. The analytic predictions do agree well with the simulations at higher η if stress concentration factors appropriate to the lattice model are used.

The remainder of this paper is organized as follows. In the next section, we describe the simulation model and the algorithm used to introduce damage according to the power-law rate of Eq. (1). In Sec. III, we present results for the general evolution of damage and failure as a function of system size and η . In Sec. IV, we compare in detail the scaling behavior found here and predicted analytically. Section V contains further discussion and a summary of our results.

II. THE SIMULATION MODEL

The use of discrete spring networks or electrical fuse networks to study failure has been quite popular over the last ten years, and is well described in many publications.³⁻⁸ Most of the studies concentrate on time-independent “fast-fracture” phenomena with a heterogeneous distribution of spring properties.^{3,4} Only a few studies, to our knowledge, have considered time-dependent damage evolution. Notable among these are the early work of Termonia and co-workers on rupture models for oriented polymer systems,⁵ and the work by Hansen, Roux, and Hinrichsen on time-dependent damage in fuse networks.⁶ These works are essentially identical in spirit and detail to the present simulations, but did not investigate the time-dependent strain evolution, the failure time, its distribution, or its size scaling in any way. These topics are the main focus of the present effort.

Here, we employ a triangular network of central force springs, each spring spanning two nodes in the triangular network.⁷ The network is subject to a fixed applied displacement by uniformly displacing the top boundary and holding the bottom boundary straight. The applied displacements are small, typically corresponding to a strain of 0.001 so that the network is always in the linear elastic range. The network is also periodic in the transverse direction. Damage in the network is represented by broken springs, or equivalently springs of zero stiffness/modulus. For any configuration of damage, mechanical equilibrium is obtained by moving all of the nodes in the network (except those on the boundaries, whose vertical coordinates are fixed by the applied displacement) to positions of zero force. This is accomplished numerically by a successive over-relaxation technique. After the equilibrium nodal positions are found, the force (“stress”) in each spring is simply the spring modulus multiplied by the net displacement difference of the nodes to which it is attached. In the present problem, the spring moduli are either a single value, which is taken as the unit of stiffness in this problem, or zero.

The applicability of discrete element models to real continuum materials requires some careful thought. For fast-fracture problems, fracture is controlled by the stress intensity factor at the microscopic tip of the crack, or equivalently the strain-energy release rate for infinitesimal advance of the

crack. In discrete models, the continuum crack tip is missing and, at best, the stress in an element ahead of a crack represents an average of the continuum stress field. The onset of unstable fracture can thus be misrepresented unless there are physical mechanisms to blunt the crack, or small cracks ahead of the crack which link up to the crack. These issues are discussed more fully by Curtin and Scher.⁷ The use of a discrete disordered structure as compared to a continuum finite-element model can lead to additional artifacts, as discussed by Jagota and Bennison.⁸

In the present problem, and the corresponding physical example of Si/SiC, the use of a spring network model can be justified. The damage that forms is not a strict slit crack, but rather a cavity, and the cavity is blunted at the ends by ductile silicon. The stress transfer around the damage is thus not highly concentrated around the tip of the damage and can reasonably be represented by the average stress across the surrounding sites. As damage clusters develop, the clusters will become more cracklike (higher aspect ratio) but still blunted; the network model can represent the enhanced stress ahead of such defects and can thus be used reliably with each spring representing a single possible damage site in the material. In application to Si/SiC, each spring would then represent a SiC/SiC grain boundary. Here, we neglect the additional presence of Si/SiC grain boundaries which do not damage as readily, and study an essentially homogeneous material composed of equivalent damage sites uniformly distributed on the lattice. We also use a regular lattice and therefore avoid the artifacts highlighted in Ref. 8. There are a few remaining artifacts of the discrete regular lattice, discussed by Curtin and Scher, which we will note as they influence the results of the simulations vis a vis the analytical predictions.⁷

Before describing the specific algorithm employed in the simulations, we first note that the problem of interest here is damage evolution under a fixed applied stress. However, for any configuration of damage the system is still linearly elastic so the relationship between stress and strain is through a time-dependent elastic modulus $E(t)$; a problem studied at constant strain can thus be easily converted to one of constant stress. As time progresses and springs are broken (replaced by zero modulus springs) the stress at fixed strain decreases, and the modulus $E(t)$ decreases concomitantly so that, at constant strain, $\sigma(t) = E(t)\varepsilon_{\text{app}}$. All of the internal stresses in the network are proportional to the macroscopic applied stress, however, because the network is linear. The situation at fixed applied stress can thus be obtained from the constant strain test by scaling all stresses by $\sigma_{\text{app}}/\sigma(t)$. Then, the strain versus time is $\varepsilon(t)/\varepsilon_{\text{app}} = \sigma_{\text{app}}/\sigma(t)$. Thus, although the numerical simulation is carried out at a fixed strain, the desired result of a fixed applied stress and increasing strain with time is easily obtained.

Now consider the damaged network at some time t , where the local stresses in the remaining undamaged springs in the network have the values $\sigma_i(t)$. Where does the next damaged site appear, and how long does it take for this event to occur? The rate of damage at any one site is as given in Eq. (1). The probability of failure $p_i(t)$ occurring at site i is thus the rate at site i relative to the total rate of damage occurring somewhere in the material,

$$p_i(t) = \frac{r_i(t)}{\sum_j r_j(t)}, \quad (2)$$

where the sum runs over all sites $1 < j < N_T$. The algorithm to pick a particular site i to fail given the probabilities $\{p_i\}$ is standard. The cumulative probability c_i , given by

$$c_i = \sum_{j \leq i} p_j(t) \quad (3)$$

is formed, and the cumulant c spans the range $[0,1]$. A random number R in the interval $[0,1]$ is then selected. The site i chosen to fail in the next interval is then the site i for which

$$c_{i-1} < R < c_i. \quad (4)$$

This procedure guarantees the selection of a site at random but consistent with the relative probabilities of Eq. (2). The average time interval required for this event to occur is simply the inverse of the sum of the rates,

$$\Delta t = \frac{1}{\sum_j r_j(t)}. \quad (5)$$

After a site is chosen to fail, the modulus of that spring is set to zero (the spring is “broken”), the time is updated by the increment Δt ,⁹ and a new state of mechanical equilibrium is determined numerically by finding the new zero-force positions for each node. The new macroscopic stress on the network, as measured by the vertical forces on the nodes at the upper boundary, is then converted to an effective macroscopic strain for the entire sample at this new time. A new damage site is then selected as described by the above algorithm.

The above algorithm of establishing the local stresses, choosing a site to fail, incrementing the time, reestablishing new local stresses, and calculating the macroscopic strain, is repeated over and over starting from the initial state of no damage, for which all nonhorizontal springs have the same tensile stress. The horizontal springs are in slight compression initially, and generally do not fail except in rare instances near the end of the test. Failure is formally defined as the point at which the strain diverges, or equivalently when the elastic modulus goes to zero. Some features of the central force network, such as free rotation of the springs around the nodes, can lead to a diverging strain even though not all of the springs in any one cross section are broken. This operationally has no effect on our simulations because we are interested in the failure time, and the diverging strain can be observed well before the network reaches complete failure, and before there are any freely rotating springs in the failure plane. Below, we will generally cease the simulations when the strain is evidently diverging, and has increased to several times its initial value.

III. RESULTS

We have investigated the evolution of strain and damage versus time in spring networks of various sizes and for a range of values of η . The size N_T of each network will be

taken as the number of springs in the nonhorizontal orientation, since the horizontal springs rarely fail, and the range of N_T studied is $264 \leq N_T \leq 28560$ for values of $\eta=2,4,8,12$. In all cases, the time scale is normalized by the reference time $1/(A\sigma_{app}^\eta)$ so that the results only depend on network size N_T and η . The initial strain is 0.001 but all results are simply proportional to the applied strain.

Figures 1(a)–1(d) show the evolution of the macroscopic elastic “creep” strain versus scaled time for one particular statistical realization at each of the values $\eta=2,4,8,12$ for various system sizes. For $\eta=2$, the damage evolution and accumulated creep strain exhibited in Fig. 1(a) are rather gradual and there is no noticeable dependence on system size except at the smallest sizes considered. Multiple realizations (not shown) indicate that the sample-to-sample fluctuations at any one fixed size are larger than the difference found for the different sizes shown in Fig. 1(a). Also, the simulations are cut off after increases of about a factor of 5 in the strain and, although increasing rapidly, there is not a sharp divergence that we will observe for higher values of η . As concluded by Hansen *et al.* in their study of the total accumulated damage at failure, the behavior of $\eta \geq 2$ is a percolation-type failure with no size dependence in any characteristics of the failure.⁶

For $\eta > 2$, distinctly different behavior occurs. Figures 1(b)–1(d) show the accumulated elastic creep strain versus system size for one statistical realization at each size for $\eta=4,8,12$, respectively. The data shown have failure times close to the mean failure time at each size. In all cases, the failure time definitely decreases with increasing system size, with a faster rate of decrease for larger η . In addition, the failure becomes more abrupt with increasing η . For $\eta=4$, there is some nonlinearity in the creep strain versus time at times as low as 50–75 % of the failure time, whereas for $\eta=12$ the deviation from linearity occurs noticeably only just before failure, at about 95% of the failure time. The failure is also increasingly abrupt with increasing size at any fixed η value. Thus, the ability to anticipate failure by monitoring damage or strain decreases both with increasing η and increasing system size.

Figures 2(a)–2(e) show the evolution of the damage for $\eta=4$ in the form of “snapshots” of the damage configurations at specific times prior to failure. In each figure, the small hash marks indicate the midpoints of springs in the triangular lattice, and so show the possible damage site locations, while the actual damaged sites are indicated by larger squares. At early times ($t \approx 0.3t_f$), the damage is limited and widely distributed with some evidence of clustering. At $t \approx 0.64t_f$, more damage and small clusters have formed but there has been no substantial growth in any individual cluster. At $t \approx 0.87t_f$, one cluster has clearly begun to grow larger, and another set of damage sites is forming an incipient connected cluster. At $t \approx 0.99t_f$ the two clusters have become dominant, and in the last 1% of life further growth occurs to form a connected cluster spanning the width of the material to cause failure. The failure at $\eta=4$ is thus controlled by the gradual development of a dominant cluster which clearly controls the failure process late in life.

Figures 3(a)–3(e) show a similar damage evolution process for $\eta=8$. Here, at $t \approx 0.55t_f$ there is very little damage with a few “dimers.” At $t \approx 0.83t_f$, there is not significantly

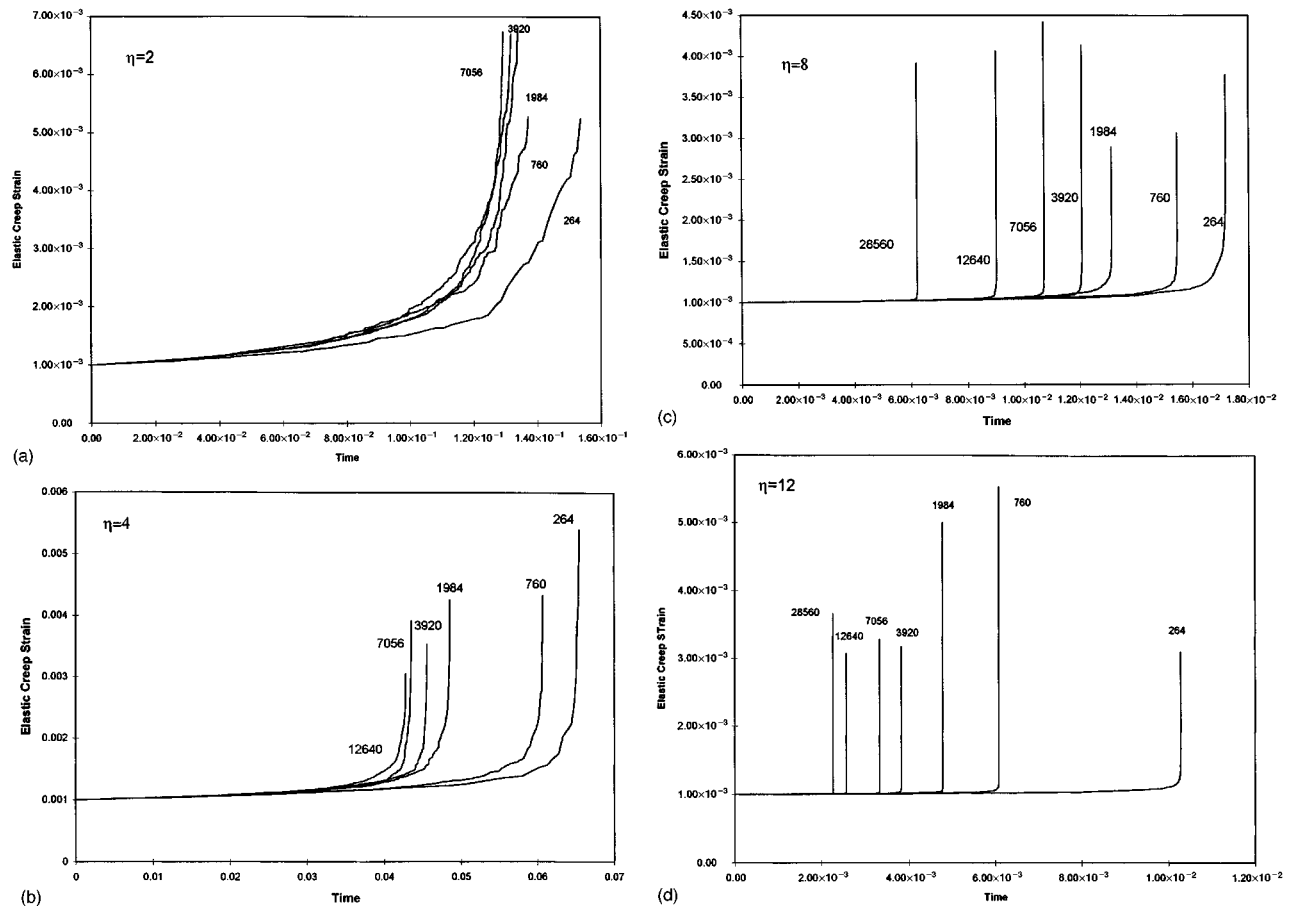


FIG. 1. Creep strain versus dimensionless time for various system sizes: (a) $\eta=2$; (b) $\eta=4$; (c) $\eta=8$; (d) $\eta=12$.

more damage but a very local region of material has preferential damage. At $t \approx 0.94t_f$, the localized damage has definitely coalesced into an extended cluster, and a few smaller clusters are formed elsewhere. At $t \approx 0.98t_f$ the dominant damage cluster is extending rapidly and now completely controls the failure, along with a secondary growing cluster. A short time later, the system is nearly spanned by a large connected cluster and the simulation was stopped. In comparison to the case for $\eta=4$, the damage for $\eta=8$ is much less in extent, and the localization occurs much more rapidly as a fraction of the total damage. This occurs, however, later in the life of the material and with less overall creep deformation, and the ultimate rapid growth to failure occurs very abruptly near the end of the life. The higher η systems are thus characterized by less damage, smaller “critical” clusters which precipitate the “avalanche” growth to failure, and consequently much more abrupt and dangerous failure.

Figures 4(a)–4(c) show the overall stress distributions in the spring networks at various times, in the form of a cumulative number of springs versus spring stress, for a size of 3680 springs at $\eta=4, 8, 12$. At early times, the distribution is nearly a δ function, and hence the cumulant is nearly a step function, because most of the sites experience the initial applied stress and no stress enhancement. As time and damage progress, the distribution broadens and the average increases, indicating the average rise in stresses on the unbroken springs due to the damage. Also, a pronounced tail at higher stresses develops, indicative of the few important springs which are under stresses much larger than the average. These

springs fail the fastest and generate larger clusters with higher stress concentrations and are the basis for the accelerating failure, as evident from the rapid growth in the high-stress tail as the failure time is approached. However, there are no distinct or characteristic features in these curves which suggest an onset of failure at any particular time, and the overall distributions exhibit no characteristic form especially in the critical tail region. Hansen, Hinrichsen, and Roux have examined the distributions of stresses just prior to complete failure (one bond left holding the entire system together) and have shown that the distribution is multifractal, but only at that one penultimate point of the evolution.¹⁰ Because of our interest here in detecting precursors to failure, and understanding the failure time, we have not analyzed the stress distribution just at failure. It will clearly be a very broad function because all of the stress is funneled through the one remaining bond, but this is not relevant to the important controlling dynamics prevailing earlier in the failure process.

IV. COMPARISON OF SIMULATIONS AND ANALYTIC PREDICTIONS

The qualitative features of the simulations found here are in general agreement with the analytic model predictions described in our previous papers.^{1,2} In particular, the failure times decrease with increasing system size for $\eta > 2$, and the failure becomes more abrupt with increasing η . Here, we wish to consider the detailed predictions of the theory re-

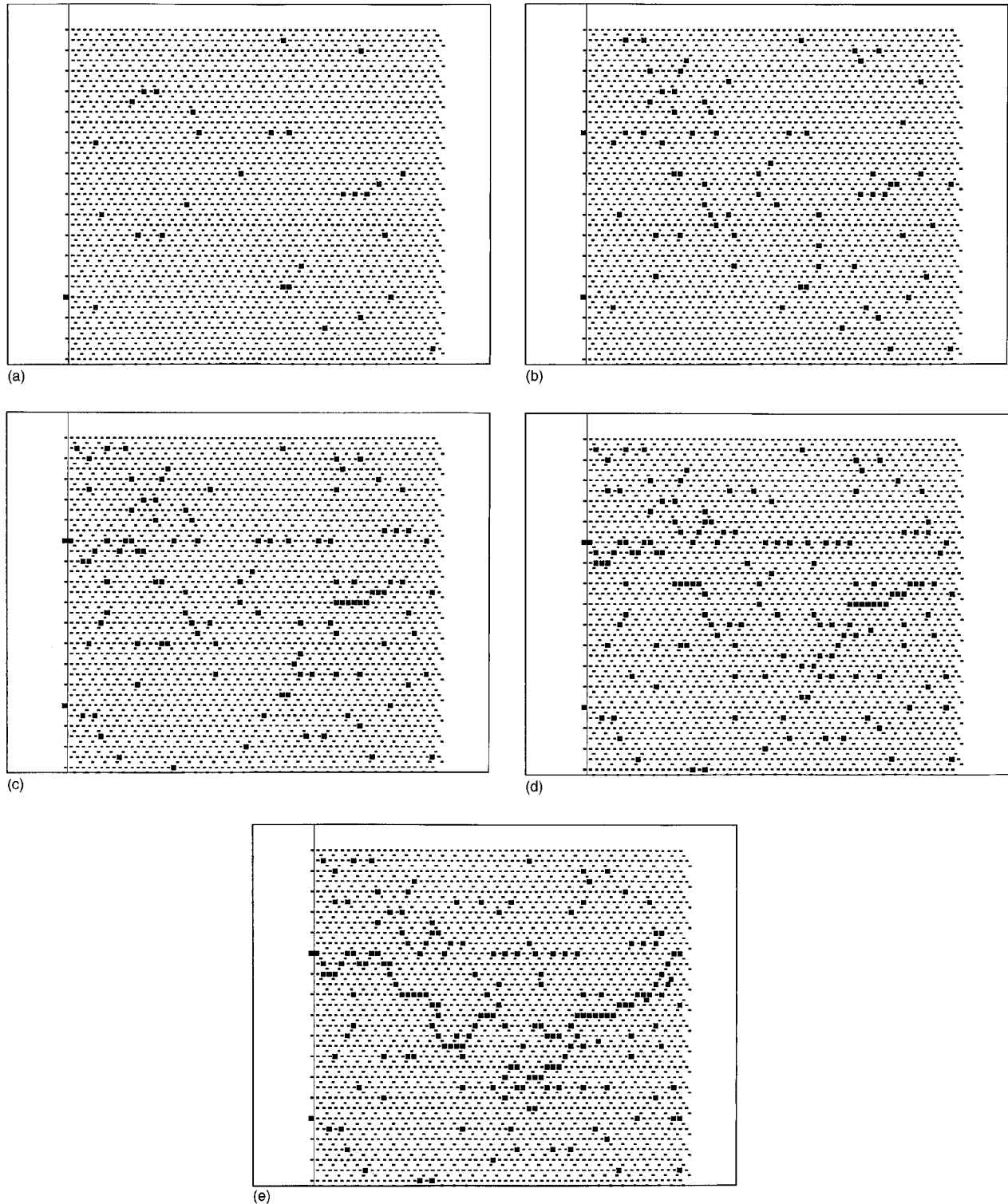


FIG. 2. Damage evolution for one particular realization at $\eta=4$, system size=1984. Small dashed lines are potential damage sites; solid squares indicate damage location. The dimensionless failure time is $t_f=0.0452$. (a) $t=0.30t_f$; (b) $t=0.64t_f$; (c) $t=0.87t_f$; (d) $t=0.99t_f$; (e) $t=t_f$.

guarding the actual scaling of the failure time and its distribution with both system size and η . The theory predicts a scaling of failure time of

$$t_f \propto (\ln N_T)^{1-\eta/2} \quad (6)$$

for systems with stress concentration factors that scales with cluster size c as $c^{1/2}$. The failure probability distribution is predicted to be (approximately) Weibull with a ‘‘Weibull modulus’’ corresponding to the critical crack size \hat{c} . For a Weibull distribution, the coefficient of variation (c.o.v.=the standard deviation divided by the mean) is reasonably repre-

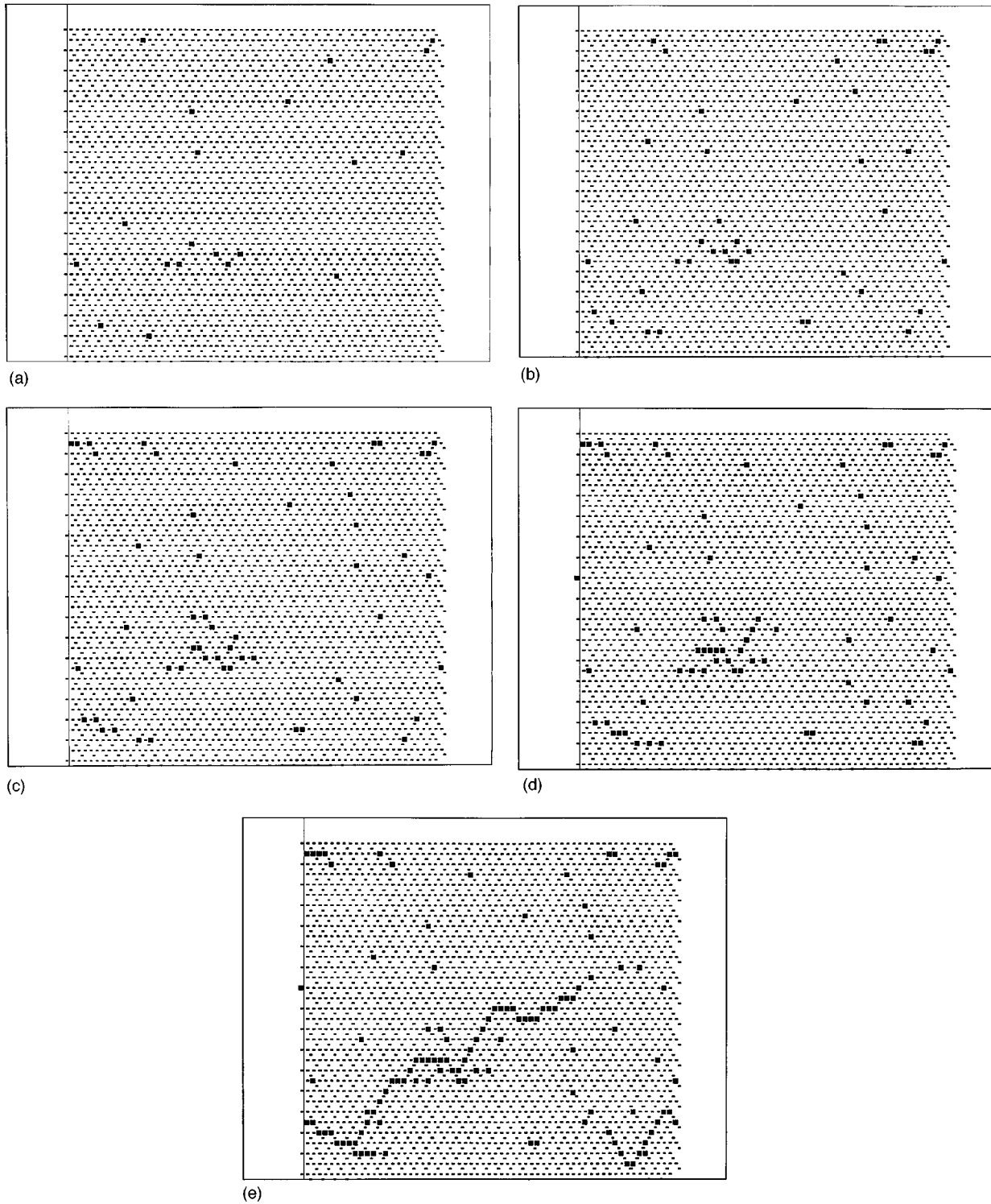


FIG. 3. Damage evolution for one particular realization at $\eta=8$, system size=1984. Small dashed lines are potential damage sites; solid squares indicate damage location. The dimensionless failure time is $t_f=0.00141$. (a) $t=0.55t_f$; (b) $t=0.83t_f$; (c) $t=0.94t_f$; (d) $t=0.98t_f$.

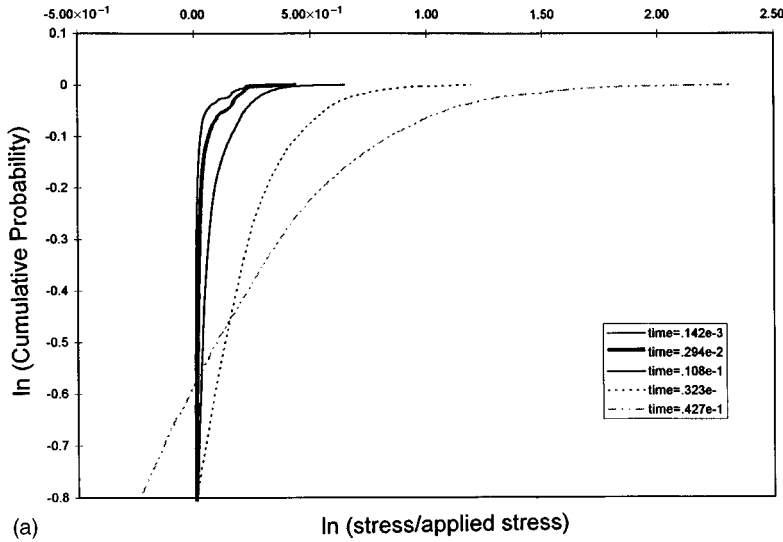
sented by $\text{c.o.v.} = 1.2/\hat{c}$. The scaling of \hat{c} and hence the c.o.v. is predicted to be

$$\hat{c} \approx \frac{\ln(N_T)}{\eta/2 - 1}; \quad \text{c.o.v.} \approx \frac{\eta/2 - 1}{\ln(N_T)} \quad (7)$$

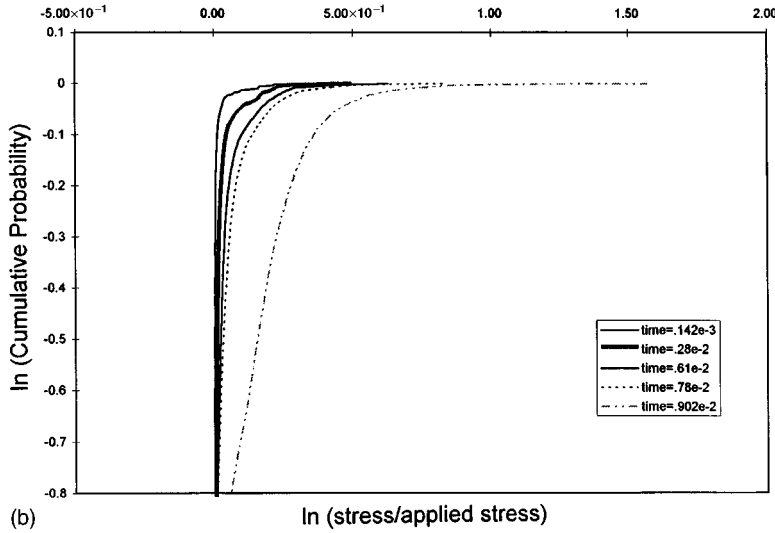
with the size scaling being independent of the value of η .

To test these specific predictions, we have performed 15

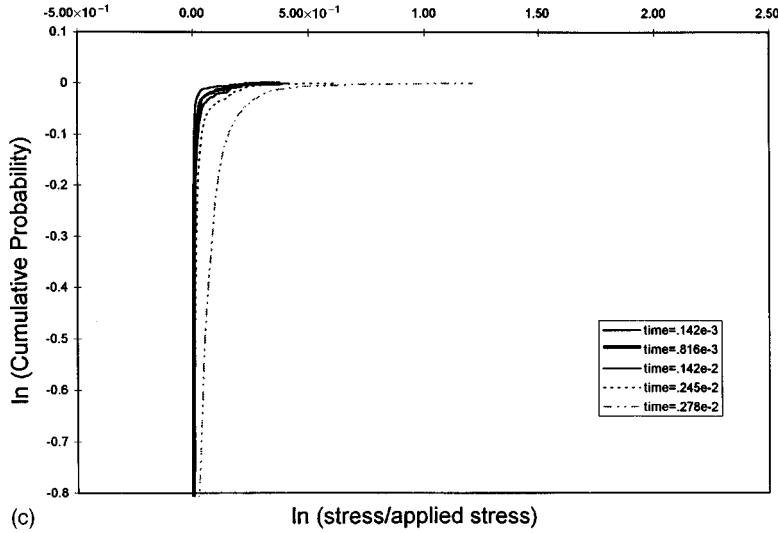
simulations at each size and at each value of η to assess the mean failure time and standard deviation of the failure time distribution. While 15 simulations is not a large number, particularly for estimating the standard deviation, the simulations are very computer intensive for larger sizes and moderate η values, and so limit our ability to collect data in the large-size regime where the dominant scalings are expected to clearly emerge.



(a)



(b)



(c)

FIG. 4. Cumulative stress distribution in damaged network versus stress, for various times up to failure for size=3620. The cumulant at stress σ is the number of springs with stress below σ , and is normalized by the total number of springs in the network, while stress is normalized by the initial applied stress. (a) $\eta=4$; (b) $\eta=8$; (c) $\eta=12$.

Figure 5 shows the failure time versus system size for the three values of $\eta=4,8,12$. The analytic model predicts a linear relationship in the $\ln t_f - \ln(\ln(N_T))$ plot, with slope $1 - \eta/2$ based on $c^{1/2}$ stress concentration factors. Figure 5 shows that over the entire range of sizes, spanning two decades in size scale, the mean failure time does scale as a

power of $\ln(N_T)$ with exponents $-0.70, -1.72,$ and -2.54 , respectively, for $\eta=4,8,12$. The corresponding predicted exponents are $-1, -3,$ and -5 , respectively, and are not close to the measured exponents.

The main reason that the predicted exponents do not agree with the simulations lies in the assumption that the stress

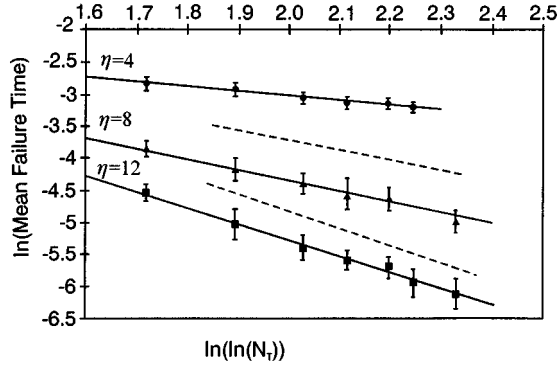


FIG. 5. Mean failure time versus system size for various η (symbols). Solid lines are the linear fit to simulation data; dashed lines are predicted from the analytic model for $\eta=8$, $\eta=12$.

concentrations are proportional to (cluster size)^{1/2}. In the discrete lattice simulation, a square-root dependence does obtain for sufficiently large cracks but at smaller crack sizes the dependence is somewhat different. Since, from the theory, the onset of failure is controlled by the initial formation of a size \hat{c} critical cluster, which then grows to failure, and since \hat{c} is fairly small for the system sizes studied here, it is conceivable that the simulations correspond to a different stress concentration factor scaling over the cluster sizes of importance. To investigate this possibility, we have introduced linear connected cracks (broken springs) of increasing size into an otherwise perfect triangular lattice and determined the stress concentration factor at the crack tips. The stress concentration factors for clusters of sizes $c=1$ to $c=8$ are shown in Table I; fits to a simple power-law dependence yield a form of $1.20c^x$ with $x=0.28-0.30$. The stress concentration factor clearly increases less rapidly than $x=0.5$. If one revisits the analytical model and replaces the exponent of $1/2$ by an exponent of x , then the scaling relationships are modified by a replacement of $\eta/2$ by ηx . For the value of $x=0.29$, the predicted exponents for the time-to-failure scaling then become -0.16 , -1.32 , and -2.48 , for $\eta=4, 8, 12$, respectively. The values for the larger η now agree reasonably with the simulations, but the value for $\eta=4$ is much too small. All the simulation results cannot be made to agree with the predictions for a single value of stress concentration factor exponent x .

The deviation at the smaller value of $\eta=4$ arises because of correlated damage evolution beyond first-near neighbors in the triangular lattice. We have analyzed the stress concentration factors at the second-neighbor sites around linear

TABLE I. Stress concentration factors at the tips of linear damage clusters versus cluster length c , in the triangular central-force spring network. Also shown is a simple power-law fit.

Length c	Stress concentration	$1.20c^x$ $x=0.28-0.3$
1	1.24	1.20
2	1.49	1.46-1.48
4	1.79	1.77-1.82
6	2.01	1.98-2.05
8	2.13	2.15-2.24

TABLE II. Probability of failure f at next-near-neighbor sites normalized by probability to fail at either near-neighbor or next-near-neighbor sites, for clusters of various lengths and various values of η . Probability is calculated following Eq. (8) of the text.

Length c	$\eta=2$	$\eta=4$	$\eta=8$	$\eta=12$
1	0.57	0.55	0.49	0.44
2	0.56	0.46	0.26	0.13
4	0.54	0.42	0.21	0.08
6	0.54	0.41	0.20	0.08
8	0.54	0.41	0.20	0.08

cracks of various sizes, and then computed the relative probabilities of failure at the near-neighbor tip sites and the next-neighbor sites as a function of η . We denote the stress concentration factor for the near neighbors as $K_{\text{NN}}^i(c)$, with $i=1-4$ for the four neighbors at the crack tip, and for the next-near neighbors as $K_{\text{NNN}}^i(c)$, with $i=1-8$, for the (typically) eight next neighbors in the triangular lattice. We then calculate the fraction

$$f = \frac{\sum_i [K_{\text{NNN}}^i(c)]^\eta}{\sum_i [K_{\text{NNN}}^i(c)]^\eta + \sum_i [K_{\text{NN}}^i(c)]^\eta}, \quad (8)$$

which is the probability that a failure will occur at a next-near-neighbor site relative to the total probability of failure at either near- or next-near-neighbor sites. This probability depends on both the decay of the stress field away from the near-neighbor tip sites and the enhancement of the probability due to the exponent η . The results for f are shown in Table II. For $\eta=2$, it is always more likely to fail away from the tip sites which prevents (generally) the development of dominant cracks in the material so that failure occurs more globally. For $\eta=4$, the fraction f is generally only slightly smaller than $1/2$ so that failure at the tips is slightly preferred but not dominant, and this feature persists out to fairly large crack sizes. However, the probability of growing at even more distant neighbors is rather smaller; hence for $\eta=4$ one must conceptually view the damage growth as occurring in a “process zone” out to next-near-neighbor distances. Although the damage does form a critical cluster locally which then grows to failure, as demonstrated explicitly in Figs. 2(a)–2(e), the failure process is not confined solely to the tips of the existing damage. The analytical model is thus not quite applicable if limited to near-neighbor interactions. For $\eta=4$, the occurrence of damage away from the crack/cluster tip sites partially corrects for the decreased probability due to weaker-than- $c^{1/2}$ stress concentration factor scaling to yield a scaling of failure time versus size that has an exponent -0.7 lying between the analytic values of -1.0 for $x=0.5$ and -0.16 for $x=0.29$.

For $\eta=8$, failure is preferred at the crack tip sites about 70–80 % of the time for clusters any larger than $c=1$. The damage evolution is thus dominated by growth of existing clusters with little damage ahead of the tips of the growing crack, and the analytic model with an appropriate exponent $x=0.29$ can account for the general scaling behavior quite

well. For the larger value of $\eta=12$, tip growth is preferred more than 90% of the time and so growth is even more dominated by the crack tip behavior, as expected. In all cases for $\eta>2$, the damage further than second-near neighbors is negligible except in accounting for the overall probability of damage at the many remote sites away from the cluster, which is already considered in the analytic model.

Overall, we see that the deviations between the simulation results and the analytic model are due to two factors: (i) a difference in the stress concentration factor at the cluster tips, which is easily accounted for in the analytic model and (ii) a longer-ranged stress-field around the clusters which can lead to damage away from the crack tip for smaller η . To account for the latter factor in the analytic model is quite difficult because one must consider as ‘‘clusters’’ sites which are not adjacent, but are separated by an intervening undamaged site for which the stress concentration factor is not well known. Models in one and two dimensions have been developed which take into account such ‘‘tapered load sharing’’ for time-independent problems, but the models are essentially statistical enumerations of all possible clusters and their associated probabilities, and are difficult to perform on ever-increasing system sizes.¹¹ The analytic model described previously can be extended to include ‘‘linking’’ of clusters separated by one adjacent site in the special case of a one-dimensional lattice, where all clusters are linear and have only $z=2$ tip sites (one at each end), but this type of model does not include the enhanced probability of failure due to longer-ranged stress fields.

Neglecting the longer-range damage for the higher $\eta=8, 12$, we can further test the applicability of the analytic model by direct calculation of the failure time distribution, using the differential equations in our companion paper and the effective stress concentration factor of $1.20c^{0.29}$. Using the full analytic differential equation includes some of the additional nonscaling terms into the overall failure time determination. The results for dimensionless failure time versus system size are also shown in Fig. 5. The predicted failure times are in good agreement with the actual simulation data in both absolute magnitude and size scaling. The predicted times are slightly longer than the simulated times, which could arise for several reasons. First, the small overall stress enhancements in the simulation accelerate the damage evolution somewhat; this effect could possibly be taken into account in the analytic model using a mean-field adjustment of the time scale but we have not found the appropriate form for carrying out this procedure accurately in the triangular lattice. In any case, as the system size increases and the total damage fraction prior to failure decreases, the average overall stress enhancements decrease concomitantly, and so the analytic results should become increasingly accurate with increasing size. This is consistent with the trends in Fig. 5. Second, the stress enhancements that do occur at the next-near-neighbor sites also accelerate the damage evolution to some extent for all system sizes, although the effect decreases with increasing η . These two considerations in tandem may explain why the agreement between theory and simulation is quantitatively the best at the largest size and largest η value tested.

Lastly, we study the failure time distribution, which controls the reliability of the material at any fixed size and fixed

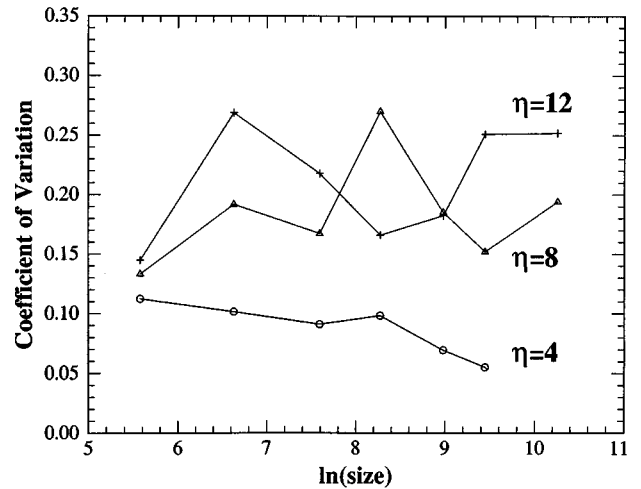


FIG. 6. Coefficient of variation of failure time distribution versus system size, for various η .

η . The theoretical model predicts that the c.o.v. should decrease as $(\ln N_T)^{-1}$ and increase with η , as indicated in Eq. (7). Since the size scaling is independent of η , it is also independent of the stress concentration factors and so a direct comparison can be made with the simulation results, as shown in Fig. 6. The simulation results are widely scattered, with the larger η values exhibiting a nearly constant c.o.v. over the entire size scale. The c.o.v. for $\eta=4$ decreases monotonically with increasing size, but the importance of next-near-neighbor damage at this η invalidates any strict comparison with the analytic prediction. In general, the c.o.v. is thus broader than predicted analytically, which implies that the theory is not conservative. This may, however, be due to the approximate analytic estimates, which were shown in the previous work to be unconservative measures of the failure distribution. The predicted trend toward larger c.o.v. with larger η is, however, exhibited in the simulation results.

If the c.o.v. values observed in the simulations for $\eta=8$ and 12 are inverted to obtain the corresponding approximate Weibull modulus of the failure distribution, one obtains estimates of the critical crack size \hat{c} varying between 5 and 9 units. The small values for the critical size \hat{c} may also lead to larger fluctuations in the simulation results than predicted analytically. For the particular case of $\eta=8$ shown in the snapshots of Figs. 3(a)–3(e), this critical crack size should set in at the onset time $\tau^*=[1-1/(0.3\eta)]\tau_f=0.58\tau_f$ using the appropriate stress concentration factors. The snapshot of Fig. 3(a) ($0.55t_f$) does not show a ‘‘cluster’’ of size approaching the average of seven units. However, at the next snapshot ($0.73t_f$) there is a ‘‘generalized’’ cluster of 4–6 units, although it is not fully connected, and it is this cluster that propagates to failure. There is not quantitative agreement between the predicted ‘‘onset’’ time and the critical cluster derived from the probability distribution width but, considering the subtleties and detail involved in such a comparison, the agreement is fair.

V. DISCUSSION

Failure processes that are triggered by a local instability are by nature very difficult to describe analytically. A com-

plete analytic prediction requires an accurate determination of the full, evolving distribution of damage and an assessment of the local stresses driving localized failure. Mean-field and averaged approaches are inappropriate, and most theoretical efforts have thus focused on idealized low-dimensional problems where the damage evolution can be exactly enumerated. Such approaches demonstrate the existence of volume-dependent failure and sensitivity to initial distributions, but are inherently precluded from extension to higher dimensions and more complex damage evolution. Hence, our present quantitative understanding of failure in heterogeneous systems that adequately represent real materials is not good. Even the direct connections between analytic models and numerical simulations have not been well established. Perhaps the state of the art is represented by the recent work of Duxbury and Leath⁴ and the earlier work of Harlow and Phoenix¹² on systems with distributed breaking strengths. They have developed recursion methods to predict failure in one-dimensional models with load transfer from breaks to near neighbors. They have demonstrated the onset of weak-link scaling at sufficiently large sizes, and Leath and Chen have shown the insidious influence of boundary conditions on the failure.¹³ However, in comparison to numerical simulations on square fuse lattices with the same initial heterogeneity, the theoretical results do not fare well quantitatively. The absolute magnitude and size scalings of the failure strengths do not match up well with the simulation results, although the qualitative trends are captured. This comparison demonstrates the difficulty in developing theories that can be solved and yet are applicable to numerical, and ultimately real, materials.

The present work has studied the problem of time-dependent damage evolution. This problem is more forgiving than the static fracture problem, in that failure is caused by the rapid but not instantaneous growth of a critical flaw which develops somewhere in the material. In addition, the damage mechanism has no memory effects which is an added simplification not generally prevailing in time-dependent problems. For this particular problem, an approximate analytic model can accurately predict the dynamics and failure of the system in a one-dimensional problem. The analytic model retains the key feature of stress transfer, and its scaling, at the tips of existing damage and neglects longer-ranged interactions. This approximation is similar in spirit to those made in the static fracture problems, but fares particularly well for the present problem under strong nonlinearity of the damage rate (high η), as demonstrated here by direct

comparison with simulation results. In particular, the transition between percolationlike and avalanche failure, and the predicted scalings and absolute values of the failure time, are in good agreement.

The generally good agreement between theory and numerical “experiment” encourages several further studies aimed toward making direct connections with experiments on real materials such as Si/SiC composites. The first challenge is to move to three-dimensional (3D) problems, where the clusters have a two-dimensional planar character. We have recently developed numerical techniques based on lattice Green functions to efficiently simulate planar damage evolution in three dimensions, and this technique will be used to gather numerical data on the 3D failure.¹⁴ Extensions of the analytic model to 3D require additional approximations because the “clusters” which could develop have a range of possible geometries and growth paths. Direct enumeration is possible for small clusters but becomes increasingly difficult as the size increases.¹⁵ Hence, new insight into the controlling growth dynamics is needed. The second challenge is to include explicit initial heterogeneity into the time-dependent failure probabilities. This can be done numerically by introducing a site-dependent rate prefactor A_i which accelerates the damage at some sites (large A_i) and retards the damage rate at other sites (small A_i). This situation does prevail in real materials, due to the effects of local microstructure and local chemistry on the damage nucleation rate. The site-dependent rate is easily introduced into the simulation models described here, and we will pursue modifications to the analytic model to understand the dynamics arising from this additional source of heterogeneity.

It is clear that to address either of the above (more realistic) problems, or other issues relevant in real materials, will require that the underlying models become much more complex. The development of approximate but accurate analytic models that capture the proper scalings, such as the model described here and in the companion paper, becomes even more critical to understanding and interpretation of the range of dynamic damage evolution and failure observed in real and model materials.

ACKNOWLEDGMENTS

The authors thank the National Science Foundation for support of this work through the Division of Materials Research, Material Theory, Grant No. DMR-9420831, and Professor S. L. Phoenix for a critical reading of the manuscript and insightful comments on the work.

¹W. A. Curtin and H. Scher, *Phys. Rev. Lett.* **67**, 2457 (1991); S. Roux, A. Hansen, and E. L. Hinrichsen, *ibid.* **70**, 100 (1993); W. A. Curtin and H. Scher, *ibid.* **70**, 101 (1993).

²W. A. Curtin and H. Scher, preceding paper, *Phys. Rev. B* **55**, 12 038 (1997).

³M. Sahimi and J. D. Goddard, *Phys. Rev. Lett.* **33**, 7848 (1986); P. M. Duxbury, P. D. Beale, and P. L. Leath, *ibid.* **57**, 1052 (1986); P. D. Beale and D. J. Srolovitz, *Phys. Rev. B* **37**, 5500 (1988); H. J. Herrmann, A. Hansen, and S. Roux, *ibid.* **39**, 637 (1989); L. deArcangelis and H. J. Herrmann, *ibid.* **39**, 2678

(1989); B. Khang, G. G. Batrounis, S. Redner, L. deArcangelis, and H. J. Herrmann, *ibid.* **37**, 7625 (1988); N. Sridhar, W. Yang, D. J. Srolovitz, and E. R. Fuller, *J. Am. Ceram. Soc.* **77**, 1123 (1994).

⁴P. M. Duxbury and P. L. Leath, *Phys. Rev. Lett.* **72**, 2805 (1994).

⁵Y. Termonia and P. Meakin, *Nature (London)* **320**, 429 (1986); Y. Termonia, P. Meakin, and P. Smith, *Macromolecules*, **18**, 2246 (1985); Y. Termonia and P. Smith, *ibid.* **20**, 835 (1987).

⁶A. Hansen, S. Roux, and E. L. Hinrichsen, *Europhysics Lett.* **13**, 517 (1990).

- ⁷W. A. Curtin and H. Scher, *J. Mater. Res.* **5**, 535 (1990).
- ⁸A. Jagota and S. J. Bennison, in *Breakdown and Non-linearity in Soft Condensed Matter*, edited by K. K. Bardhan, B. K. Chakrabarti, and A. Hansen (Springer-Verlag, Berlin, 1994).
- ⁹In principle, the elapsed time is statistically distributed around Δt , and so should be chosen randomly from an exponential distribution $\exp(-t/\Delta t)$. However, since many time steps are taken prior to failure, the fluctuations in the total elapsed time due to the statistical variations in individual time steps decrease rapidly according to the central limit theorem and can therefore safely be neglected.
- ¹⁰A. Hansen, E. L. Hinrichsen, and S. Roux, *Phys. Rev. B* **43**, 665 (1991).
- ¹¹R. E. Pitt and S. L. Phoenix, *Int. J. Fract.* **22**, 243 (1983).
- ¹²D. G. Harlow and S. L. Phoenix, *Int. J. Fract.* **17**, 601 (1981).
- ¹³P. L. Leath and N. N. Chen, in *Damage Mechanics and its Applications*, edited by J. W. Willis (Kluwer, Dordrecht, 1996).
- ¹⁴W. A. Curtin, *J. Am. Ceram. Soc.* **78**, 1313 (1995).
- ¹⁵R. L. Smith, S. L. Phoenix, M. R. Greenfield, R. B. Henstenburg, and R. E. Pitt, *Proc. R. Soc. London Ser. A* **388**, 353 (1983).